Organic Process Research & Development

ARTICLE

pubs.acs.org/OPRD

Use of *in Situ* Raman, FBRM, and ATR-FTIR Probes for the Understanding of the Solvent-Mediated Polymorphic Transformation of II−I Etiracetam in Methanol

Christelle Herman,[†,*] Benoît Haut,[†] Sélim Douieb,[†] Aurélie Larcy,[†] Valérie Vermylen,[‡] and Tom Leyssens[§]

[†]Université Libre de Bruxelles, Transfers, Interfaces and Processes Department, Chemical Engineering Unit, 50 Avenue Franklin D-Roosevelt, CP 165/67, 1050 Bruxelles, Belgium

[‡]UCB Pharma, 60 Allée de la Recherche, 1070 Braine l'Alleud, Belgium

[§]Université Catholique de Louvain, Institute of Condensed Matter and Nanosciences, 1 Place Louis Pasteur, 1348 Louvain-La-Neuve, Belgium

Supporting Information

ABSTRACT: The objective of the present paper is to show the utility of combining distinct online and *in situ* probes, tracking both the solid and the liquid phases, to come to a full understanding of the mechanism underlying polymorphic transformations. The study focuses on the batch crystallization process of etiracetam (racemic intermediate to the synthesis of levetiracetam [Keppra, UCB Pharma], presenting two enantiotropically related crystallographic forms) in methanol, as this process relies on a polymorphic transformation in solution prior to the isolation of the final compound. The polymorphic transformation is shown to follow a solvent-mediated polymorphic transformation mechanism, which is characterized by three successive phases. Identification and understanding of each of these phases requires the knowledge on the nature of the crystallographic form (Raman probe), the variations in particle size distributions (FBRM probe) as well as the solute concentration in solution (ATR-FTIR probe), showing the necessity of combining these different online analyzers.

1. INTRODUCTION

1.1. Polymorphic Transformations. One of the most frequently used industrial processes to achieve the required purity of active pharmaceutical ingredients (APIs) combines a solution crystallization operation, often by cooling, with a separation of the obtained crystals from the mother liquid.[1,2] Frequently, the development of crystallization processes still relies on an empirical trial-and-error approach, which does not always yield a robust and optimized process. Furthermore, a lack of process understanding may lead at later stages (scale-up or production) not only to process-related issues (e.g., caking, difficulty to determine the end point of the process, etc.) but also to inconsistency in the quality of the product. One such quality attribute, depending on the crystallization conditions, is the final crystallographic form of the solid crystals.[3] Especially for APIs, this form is of importance to avoid stability, solubility, or bioavailability issues. Moreover, it is not uncommon to observe the appearance of several crystallographic forms during a crystallization process. To ensure the crystallographic form of the final product, it is of importance to understand the physicochemical phenomena underlying the formation of the different crystallographic forms and the mechanism of the polymorphic transformation leading from one form to another.

Trying to understand the transformation of one form to the other can, in principle, be achieved through sampling and offline analysis, although this is tedious and often leads to a limited insight into the polymorphic transformation process, due to the complexity of this latter. Over the recent years, important advances have therefore been made in analyzing the process *in situ* using online process analyzers. The quality by design (QBD) guideline of the U.S. Food and Drug Administration (FDA) encourages the use of process analytical technology (PAT); online *in situ* probes such as focused beam reflectance measurement (FBRM), particle vision and measurement (PVM), Raman, attenuated total reflectance Fourier transformed infra-red (ATR-FTIR) or near infra-red (NIR) probes are nowadays becoming common tools for process development.[4] Using these techniques, sampling is avoided and 'on the fly' information can be obtained. In turn, this can be directly related to changes occurring in the process.

For solvent-mediated polymorphic transformation studies, many applications have been developed involving a single PAT measurement probe: ATR-FTIR,[5] NIR,[6] Raman,[7] or FBRM.[8,9] Although the use of a single measurement probe can give valuable insight into the process, understanding of complex process mechanisms often requires the simultaneous use of different probes. The feasibility of using a FBRM probe to monitor changes in the morphology of the crystals in conjunction with a PVM probe[10] and a Raman spectroscopic probe[11] has been reported in literature. For the purpose of understanding the crystallization process and, more specifically, a polymorphic transformation, it is important not only to gain information on the solid states appearing in the suspension but also to

Received: June 24, 2011
Published: October 24, 2011

understand variations in solute concentration in solution. Understanding such a transformation mechanism would therefore require combining probes such as FBRM and ATR-FTIR,[12] Raman and NIR,[9] FBRM, PVM, Raman, and ATR-FTIR.[13] The objective of this paper is to show how the information gained from three different *in situ* and online tools (Raman, FBRM, and ATR-FTIR) can be combined to come to a full understanding of the mechanism underlying a solvent-mediated polymorphic transformation.

1.2. Study Case. The stirred tank cooling crystallization of etiracetam in methanol was chosen as a study case, as this process relies on a polymorphic transformation in solution prior to the isolation of the final compound.

Etiracetam (Figure 1) is encountered as a racemic intermediate in the synthesis of levetiracetam, the active ingredient of Keppra, an antiepileptic drug commercialized by UCB Pharma. Etiracetam can crystallize in two distinct crystallographic forms, form I (Figure 2a) and form II (Figure 2b), which are enantiotropically related. As shown in previous works, techniques such as differential scanning calorimetry (DSC),[14] Raman spectroscopy (Figure 3a),[15] X-ray powder diffraction (XRPD) (Figure 3b), or granulometry[16] can be used to distinguish the two crystallographic forms. The solubility of the two forms of etiracetam in methanol has been determined experimentally by combining five different experimental techniques.[17] The form I and form II solubilities (expressed in grams of solute per gram of solution: g/g_{sol}.) are presented in black and grey, respectively, in Figure 4. The transition temperature of this polymorphic system is equal to 30.5 °C: form I is the stable crystallographic form below 30.5 °C, while form II is the stable crystallographic form beyond 30.5 °C.[15]

The crystallization process of etiracetam, adopted by UCB Pharma, is a batch-cooling solution crystallization which starts by the dissolution of crude etiracetam in methanol at an initial etiracetam concentration in solution of approximately 0.6 g/g_{sol}. A 1 h isothermal hold at 60 °C assures that the compound is entirely dissolved. The crystallization process can be divided into two successive steps: the cooling step and the so-called maturation step. Subsequent cooling of the solution from 60 °C occurs at 15 °C/h and is jacket-controlled. During cooling, the compound crystallizes. Offline analysis (DSC, Raman, XRPD, etc.) shows that the crystals formed are of form II. The final suspension is then left overnight at a constant maturation temperature (T_{mat} < 30.5 °C), close to 0 °C. During this maturation step, a polymorphic transformation occurs, leading to form I, which is of interest from a pharmaceutical point of view. The presence of this new crystallographic form is confirmed by offline analysis.

Although being used on a large scale, the actual mechanisms underlying the crystallization process of etiracetam (and more specifically the polymorphic transformation) were not well understood. This contribution shows how different online tools are combined to come to a full understanding of the etiracetam polymorphic transformation mechanism, combining three distinct online and *in situ* probes, tracking both the solid and the liquid phases.

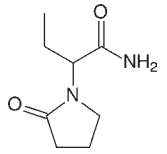

Figure 1. Molecular structure of the etiracetam compound.

2. METHODS

All crystallization experiments were carried out in a 2-L automated Mettler Toledo Labmax reactor. Three online and *in situ* analytical probes were inserted in the reactor (Figure 5): Raman, FBRM, and ATR-FTIR probes (Supporting Information [SI]). The Raman spectroscopic probe (Horiba Jobin Yvon, LabRam Aramis, Super Head probe, optical fibre conduct) has a typical laser power of 200 mW at 785 nm, with exposure time for the measurement set at 2 min. The FBRM probe (Lasentec, Mettler Toledo, D600L), allows for chord lengths to be measured within a 1−1000 μm range with exposure time for the measurement set at 2 s. These two probes allowed for tracking over time the properties of the solid phase, i.e. the nature of the crystallographic form and the chord length distribution of the suspended crystals, respectively. The ATR-FTIR probe (Mettler Toledo, ReactIR4000, diamond dicomp 16-mm tip, K6 conduct) has exposure time for the measurement set at 5 min. A partial

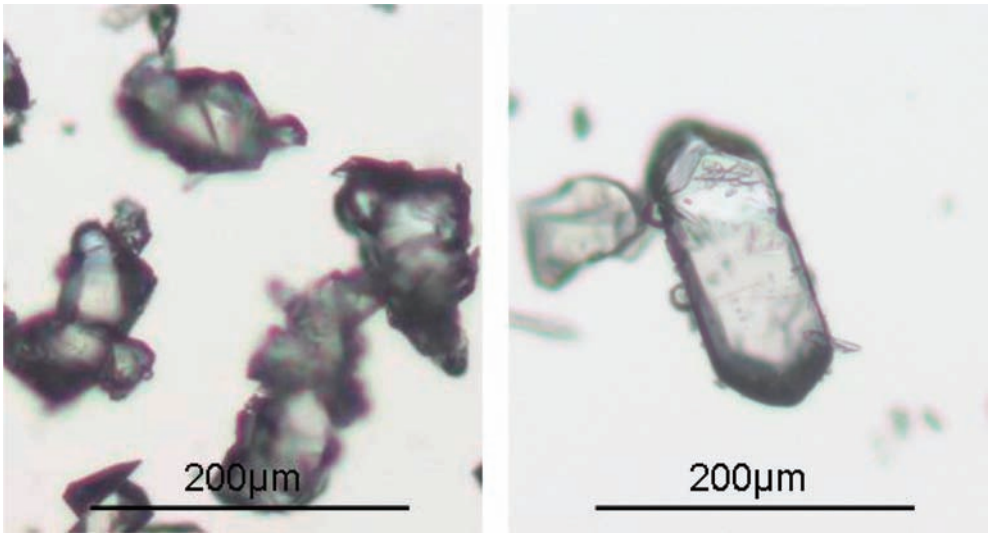

Figure 2. Optical microscopy picture of (a) form I crystals and (b) form II crystals.

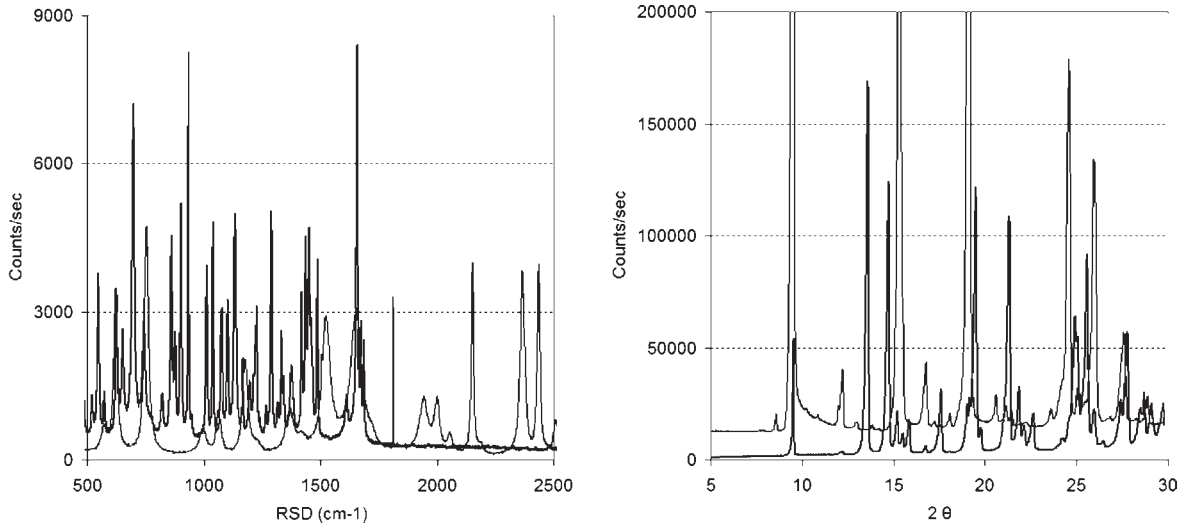

Figure 3. (a) Raman spectra (Horiba Jobin Yvon, LabRam Aramis, 120 s exposure time at 785 nm[15]) and (b) XRPD pattens (Bruker B8 Advance diffractometer, monochromatic Cu radiation[16]) of the form I crystals (black line) and the form II crystals (grey line) (RSD: raman shift displacement).

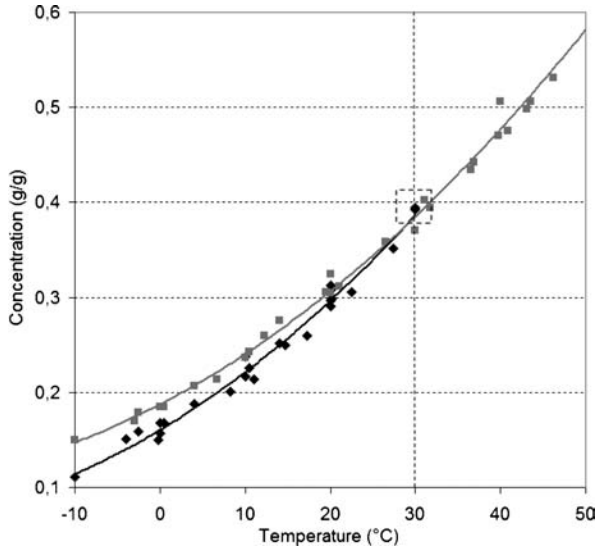

Figure 4. Experimental solubilities (points), as well as polynomial second-order regressions (curves), of both form I crystals (black line) and form II crystals (grey line) in methanol. The transition temperature is estimated at 30.5 °C.

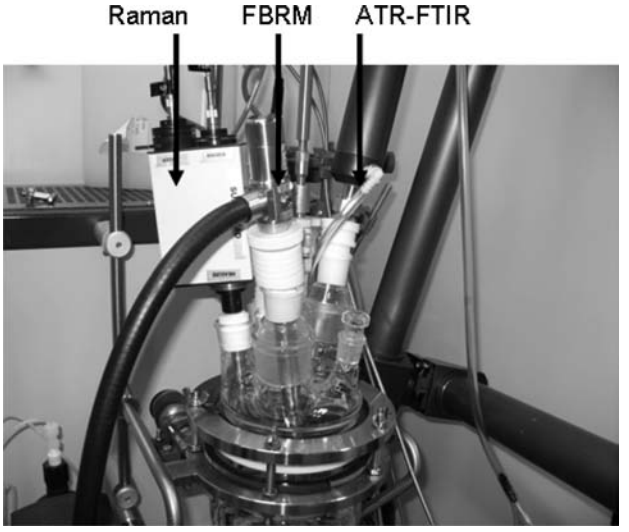

Figure 5. Two-liter automated Mettler Toledo Labmax reactor instrumented with online *in situ* Raman, FBRM, and ATR-FTIR probes.

least squares calibration model was used to relate the IR signal to the etiracetam concentration in solution (SI). Mass temperature was also recorded online over time

For each experiment, crude etiracetam and methanol were added to the reactor to obtain an initial concentration of 0.57 gram of etiracetam per gram of solution (0.57 g/g_{sol}). Stirring was ensured by a Mixell TT glass impeller rotating at 400 rpm, chosen in order to obtain a dissipated power per unit volume of the suspension equal to the one in the industrial vessel. The cooling rate was jacket-controlled and fixed at 15 °C/h. The nature of the polymorphic transformation mechanism is assumed to be independent of the maturation temperature, provided that this temperature is below the transition temperature (30.5 °C). For the purpose of this work, the maturation temperature was fixed at 10 °C. This temperature was found to lead to an optimal data acquisition for all three probes; while a sufficient density of crystals was required for the Raman probe, a too high density of solid particles in suspension interfered with the ATR-FTIR probe (SI). Finally, it is also assumed that the insertion of PAT analysers do not influence the nature of the polymorphic transformation mechanism.

3. RESULTS

In this section, the overall data obtained from the different online probes are presented, followed, in the next section, by a detailed discussion of the two steps (cooling step and maturation step) of the crystallization process. A total of four experiments have been realized, all leading to similar observations. The time evolution of the temperature and of the signals recorded by the three online probes is presented in Figure 6, for one of these four experiments.

The time evolution of the temperature during the process is presented by a continuous dark grey line in Figure 6, clearly showing the cooling step, during which the temperature decreases from 60 to 10 °C, followed by the maturation step, characterized by an isothermal hold at 10 °C. Two exothermic peaks are observed on the temperature profile, the first one appearing after 1 h at approximately 45 °C (Figure 7a) and the second one appearing during the isothermal hold after approximately 12 h. The temperature oscillation observed after this second peak is due to the ID temperature regulator of the automated Labmax reactor. The time period between the beginning of the cooling step and the onset of the first exothermic peak will be referred to as the crystallization time and written t_{cryst}. The time period between the beginning of the maturation step and the maximum of the second exothermic peak will be referred to as the latency time and written $t_{latency}$.

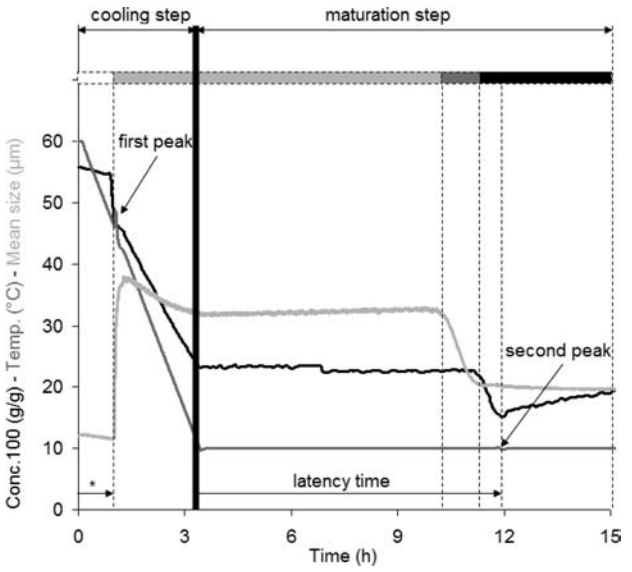

Figure 6. Time evolution of the etiracetam concentration in solution, the temperature of the solution, the mean size of the suspended crystals and the nature of their crystallographic form (in the upper box: white = no crystal, light grey = form II, dark grey = mixture of both forms, black = form I). Conc. = concentration, Temp. = temperature, * = crystallization time. The values of the concentration are multiplied by 100 for a better representation of all data in the same figure.

The most useful part of the Raman spectra allowing a distinction between the two crystallographic forms of the suspended crystals extends from 1300 to 1400 cm^{-1}. Particularly, suspended form I crystals show two significant peaks at 1340 and 1375 cm^{-1}, while suspended form II crystals show three significant and distinct peaks at 1332, 1353, and 1382 cm^{-1}, respectively.[17] The crystallographic form of the suspended crystals, as observed by the Raman probe, is presented in the upper box in Figure 6. This upper box is highlighted according to the nature of the crystals in the suspension: light grey corresponds to form II crystals, black corresponds to form I crystals, and dark grey corresponds to a mixture of both crystallographic forms. The white color is used when no crystals are detected in suspension.

A lot of process insight can be gained from analysis of the chord length distributions (CLD) recorded by the FBRM probe over time (SI). One such statistical parameter considered in this work, presented by a continuous light grey line in Figure 6, is the mean size of the crystals in suspension. The chord counts per second (counts/s) in four crystal size intervals are also presented in a and b of Figure 8 (class 1 - fine: 1 at 12 μm, class 2 - fine: 11 at 39 μm, class 3 - medium: 36 at 117 μm, class 4 - coarse: 109 at 288 μm).

The continuous black line in Figure 6 represents the time evolution of the etiracetam concentration in solution extracted from the ATR-FTIR signal.

4. DISCUSSION

In this section, the data obtained using the different probes are combined to understand the underlying crystallization mechanisms occurring respectively during the cooling step (Figure 9a) and maturation step (Figure 9b).

4.1. Cooling Step. As shown, the crystallization time, as defined previously ($t_{cryst} \approx 1$ h), coincides with the detection of the first crystals by the FBRM and the Raman probes. Before $t = t_{cryst}$, only a background noise signal is detected by the FBRM probe. At $t = t_{cryst}$ the counts/s in the four classes drastically increases (Figure 8), indicative of a drastic increase of the number of crystals in suspension. This increase is also observed in the time evolution of the mean size of the crystals (Figure 9a). Raman analysis indicates the formation of form II crystals. The solution temperature at $t = t_{cryst}$, commonly called the

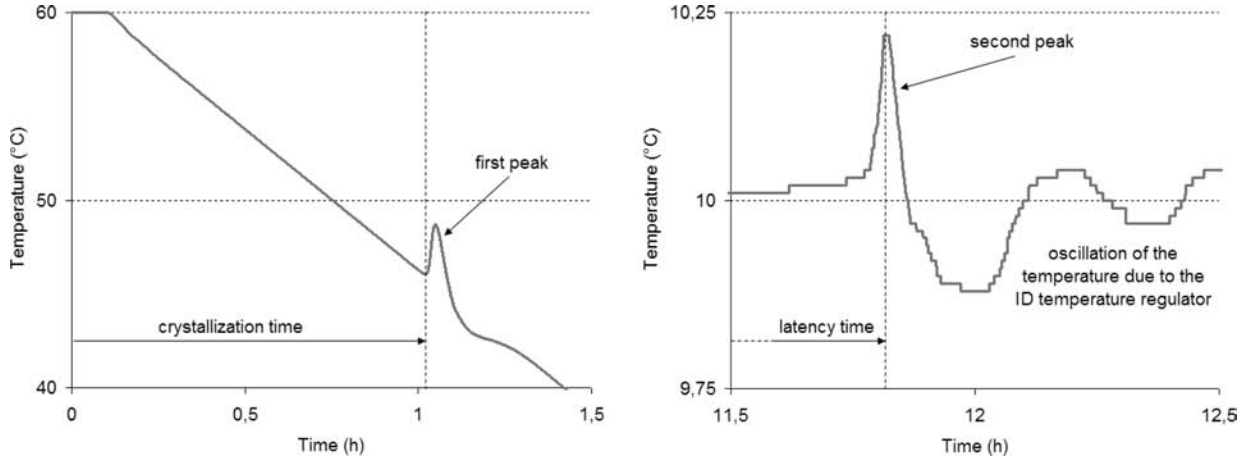

Figure 7. Presence of (a) a first exothermic peak during the cooling step and (b) a second exothermic peak during the maturation step.

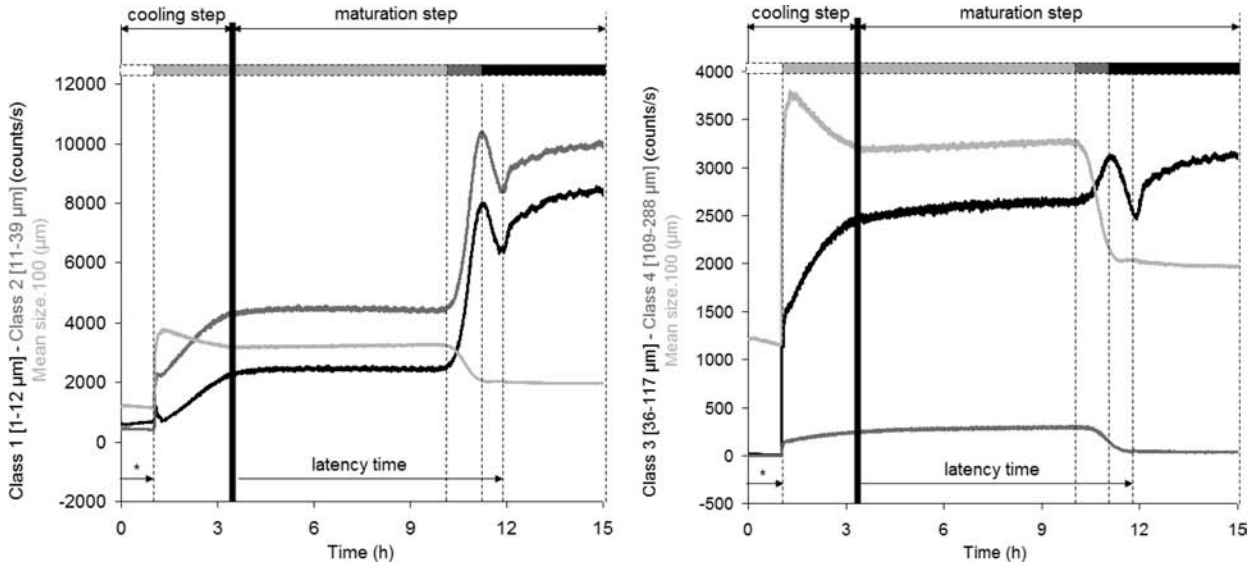

Figure 8. Time evolution of the chord counts/s in (a) the two smallest particles classes and (b) the two largest particles classes. Mean size of the suspended crystals and nature of their crystallographic form (in the upper box: white = no crystal, light grey = form II, dark grey = mixture of both forms, black = form I).* = crystallization time. The values of the mean size are multiplied by 100 for a better representation of all data in the same figure.

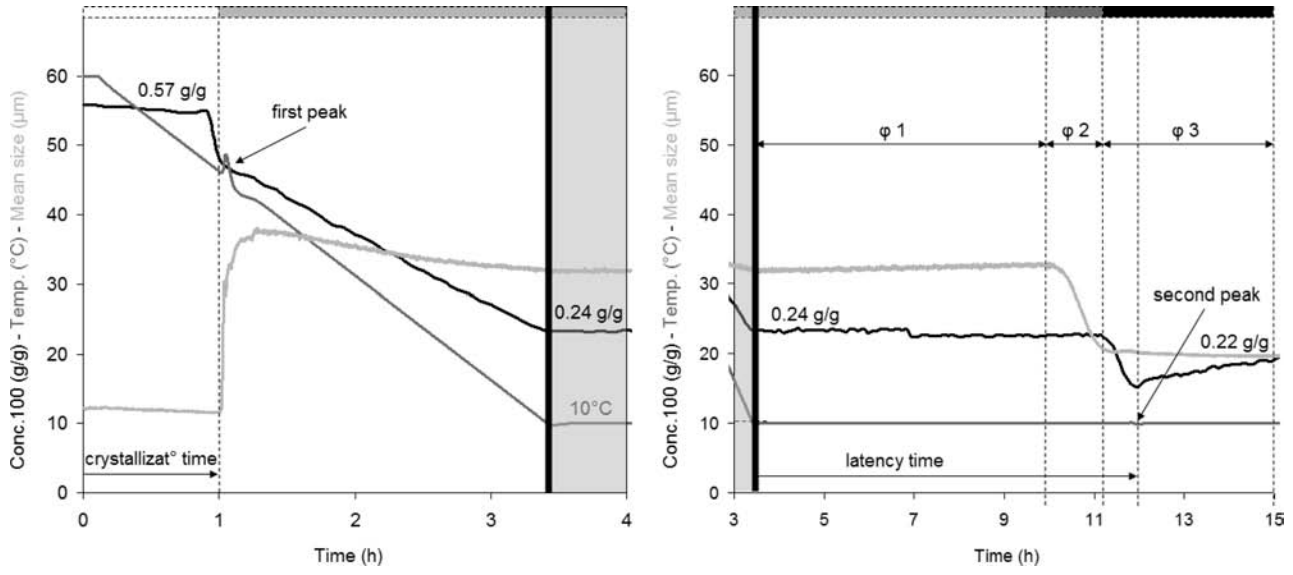

Figure 9. Time evolution of the etiracetam concentration in solution, the temperature of the solution, the mean size of the suspended crystals and the nature of their crystallographic form (in the upper box: light grey = form II, dark grey = mixture of both forms, black = form I) during (a) the cooling step and (b) the maturation step. Conc. = concentration, Temp. = temperature, φ = phases of the maturation step (detailed in section 4.2). The values of the concentration are multiplied by 100 for a better representation of all data in the same figure.

crystallization temperature, lies below the thermodynamic solubility temperature (~50 °C). This crystallization temperature limits the metastable zone, whose width essentially depends on the hydrodynamic conditions in the 2-L reactor.[35,36] Although not detected by the FBRM and the Raman probes, microscopic crystals are expected to be present in suspension just before $t = t_{cryst}$ (or just before $T = T_{cryst.}$). This is confirmed by the observed slight decrease of the etiracetam concentration in solution before $t = t_{cryst}$ (Figure 9a). At $t = t_{cryst}$ the solution concentration lowers instantly. This sudden appearance of particles as well as substantial drop in the etiracetam concentration in solution, occurring during a relatively reduced time interval (i.e., $t = t_{cryst} \pm 3$ min), is characteristic of an initial spontaneous crystallization. As the transformation from dissolved to solid state is exothermic, a temperature increase is observed after $t = t_{cryst}$ (Figures 7a and 9a).

After $t = t_{cryst}$ (or $T = T_{cryst.}$), further cooling leads to a rapid consumption of the supersaturation by crystal growth and/or secondary nucleation, leading at all times to an etiracetam concentration in solution that is approximately equal to the form II solubility (Figure 10). The increase in number of large particles (Figure 8b) confirms crystal growth occurs during the entire cooling stage. The increase in number of small particles (Figure 8a) can be attributed either to secondary nucleation, to

dx.doi.org/10.1021/op200168g |*Org. Process Res. Dev.* 2012, 16, 49–56

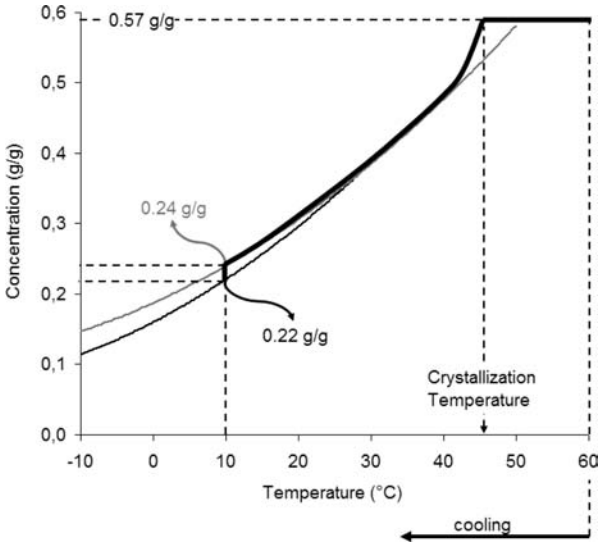

Figure 10. Solubilities of form I (black line) and form II (grey line) as well as the temperature evolution of the etiracetam concentration in solution during the crystallization process (bold black line).

breaking or attrition of the larger crystals. Below the solid−solid transition temperature (30.5 °C), the solution is supersaturated with respect to form I crystals (Figure 4). Nevertheless, no form I crystals are detected by the Raman probe (Figure 9a), which is most likely due to the low nucleation rate of the form I crystals. After 3 h and 20 min, the temperature of the form II suspension reaches the maturation temperature of 10 °C. The etiracetam concentration in solution stabilizes at the form II solubility at 10 °C (0.24 g/g_{sol}) (Figures 9a and 10). The mean size of the suspended form II crystals and the crystal counts/s in each class of the CLD stabilize at this stage (Figure 9a).

During cooling, a spontaneous crystallization of form II crystals is thus observed. Although no polymorphic transformation occurs during cooling, the data obtained from the online probes gives valuable insight into this first step of the process, and confirms the presence of a single crystallographic form after initial crystallization.

4.2. Maturation Step. At 10 °C, the so-called maturation step starts during which the polymorphic transformation occurs as will be shown later on.

The concept of using particle size analysis to determine the mechanism of polymorphic transformation has been reported since 1985.[37] The particle size distribution (PSD) of the suspended crystals either will essentially remain unchanged during the polymorphic transformation if this latter proceeds via a solid-state transformation or will change to a more significant extent if the polymorphic transformation occurs through a solvent-mediated transformation. Monitoring the PSD over time during an isothermal hold can therefore allow identifying the nature of the polymorphic transformation mechanism, provided that the PSD of the stable and the metastable crystals are significantly different[9] and assuming that no other phenomenon (breaking, attrition, agglomeration, secondary nucleation, etc.) interferes with the polymorphic transformation and affects the PSD of the crystals. Figure 8 shows significant changes to occur in the FBRM population statistics about 10 h into the maturation step. As shown later on, at this stage a change in crystal form occurs, and the FBRM data thus indicate the transformation mechanism from the metastable form II crystals towards the stable form I crystals to be a solvent-mediated, polymorphic transformation mechanism.

Such a transformation typically involves three phases, which are presented in Figure 9b:[7,38−40] (φ 1) nuclei of the most stable form appear in suspension, a process driven by the supersaturation with respect to this form; (φ 2) these nuclei start to grow, and the crystals of the metastable form simultaneously dissolve; (φ 3) once all of these latter are completely dissolved, the crystals of the stable crystallographic form grow until the equilibrium etiracetam concentration of stable form in solution is reached. Each of these phases will be studied separately in detail hereafter, on the basis of the data obtained using the three probes.

The first phase (φ 1) starts at the onset of the maturation step. The solution is supersaturated with respect to form I (Figures 4 and 10). From a thermodynamic point of view, form I nuclei are therefore expected to appear in suspension. However, the Raman probe does not detect any such crystals, most likely due to the limited number and size of these crystals. Moreover, the etiracetam concentration in solution remains equal to the form II solubility (0.24 g/g_{sol} at 10 °C). The slight increase of the mean size of the crystals in suspension is attributed to the Ostwald ripening process of the form II crystals. This first phase (φ 1) ends when the form I crystals reach a sufficient size that allow their detection by the PAT analysers. The time up to the detection of these first crystals can be divided into the following three characteristic times: (i) a nucleation time, during which the first nuclei appear; (ii) a growth time, during which the nuclei, previously formed, grow; and (iii) a latency time, corresponding to the time needed for the crystals to become sufficiently large for the PAT analysers to be able to detect them.[1,2] As the former two are quite substantial, it takes approximately 10 h into the maturation zone before any significant change is observed in the etiracetam suspension characteristics.

The second phase (φ 2) starts from the moment form I crystals are detected by the FBRM and the Raman probes. During the entire duration of the second phase, the Raman probe detects form I and form II crystals in suspension (Figure 9b, upper box highlighted in dark grey). During this second phase, the form I crystals consume the form I supersaturation, most likely both through crystal growth, as well as through secondary nucleation. As the etiracetam concentration in solution now drops slightly below the metastable form II solubility, the form II crystals start to dissolve. In the case of etiracetam in methanol, the etiracetam concentration in solution remains slightly less than the form II solubility, indicating the global dissolution of form II crystals to occur more rapidly compared to the overall mass increase of form I crystals.[39,40] Mass increase of form I crystals, and dissolution of form II crystals is illustrated by the FBRM data shown in Figure 8. The increase of the crystal counts/s of classes 1 up to 3 can be attributed to the number increase of the small form I crystals either by growth or by secondary nucleation while the decrease of the crystal counts/s of the fourth class is indicative of the dissolution of the form II crystals previously formed. The sum of these phenomena results in an overall decrease of the mean crystal size.

The third phase (φ 3) starts when the crystals of form II are totally dissolved.[39,40] At this stage, the Raman probe only detects form I crystals in suspension (Figure 9b: upper box highlighted in black). As there are no form II crystals left to dissolve, form I crystals consume the remaining supersaturation with respect to this form, leading to the decrease of the etiracetam concentration

in solution (Figure 9b). The consumption of the supersaturation mainly occurs by form I growth. This exothermic phenomenon is accompanied by a temperature increase of the suspension, which is translated in a second exothermic peak. This peak was previously used to define the latency time (Figure 9b). As can be observed, form I crystals are already present one hour before the maximum of the exothermic peak. It might therefore be advisible to omit the notion of latency time and instead use the notions of onset and endset of polymorphic transformation to indicate respectively the beginning of φ 2 and the end of φ 3. Using the second exothermic peak for process control can furthermore be quite difficult due to the small amplitude of the temperature variation ($\Delta T \approx 0.5$ °C). To detect the different phases of the polymorphic transformations, and hence control the overall process, the use of online and *in situ* Raman, FBRM, and ATR-FTIR probes is recommended. Moreover, the consumption of the supersaturation is accompanied by a mass increase of the suspended crystals. Unfortunately, this information cannot be verified directly through the use of the online probes. However, it has been shown elsewhere that the second exothermic peak occurs simultaneously with the increase of the apparent viscosity of the suspension, which was shown to be related to the increase of the volume—or mass—fraction of the form I crystals in suspension.[16] At the onset of φ 3, all CLD classes indicate a sudden decrease in particle counts/s, which is most likely due to the slight increase in temperature during the second exothermic peak (Figure 8) and due to the modification of the jacket temperature by the ID temperature regulator of the automated Labmax reactor with the aim to maintain the temperature of the suspension at 10 °C. These unphysical minimum values of particle counts/s are reached at the latency time, corresponding to the maximum of the second exothermic peak. All classes show, then, an increase in particle counts/s until stabilizing once the temperature is brought back to 10 °C, corresponding to the endset of the second exothermic peak. The strong fluctuation in etiracetam concentration in solution at the onset of φ 3, with an unphysical concentration lower than the equilibrium form I concentration in solution, can possibly also be attributed to perturbations in the ATR-FTIR analysis due to the sudden temperature variations, or due to a burst in microsized crystals possibly interfering with or crystallizing on the probe.[2] Additional experimental work to fully understand the effect of the temperature on the three phases identified above is currently ongoing and will be published elsewhere. After total consumption of the form I supersaturation, all suspension characteristics stabilize, with the mean particle size of the form I crystals being smaller than that of the form II crystals. The etiracetam concentration in solution stabilizes at the etiracetam form I solubility (0.22 g/g_{sol} at 10 °C) (Figures 9b and 10).

As highlighted by Figure 9b, φ 1 is the limiting phase for the solvent-mediated polymorphic transformation from the metastable form II towards the stable form I. Experiments performed at lower maturation temperatures (−2 °C and −10 °C) show the duration of this phase to decrease with respect to a decrease in suspension temperature. At a temperature of −10 °C, the total process time can be reduced by about 5 h. For the etiracetam case studied here, the shorter φ 1 at lower temperatures can be understood by the increase in supersaturation with respect to the most stable form at lower temperatures (Figure 4) and hence an increase in form I nucleation and crystal growth rates. Additional experimental work to fully understand the effect of the temperature on the three phases identified above is currently ongoing, and will be published elsewhere. More than the maturation temperature, others factors — which are not studied in this work — may also govern the rate of solvent-mediated polymorphic transitions, such as the degree of agitation, the nature of the solvent, the presence of impurities, the seeding with crystals of the stable form, etc.[41]

5. CONCLUSION

In this contribution, the utility of combining different online and *in situ* probes to arrive to process understanding is illustrated. More specifically, Raman, FBRM, and ATR-FTIR probes are combined in order to understand the underlying process mechanism of the polymorphic transformation occurring during the etiracetam crystallization process in methanol. The polymorphic transformation at maturation temperature is shown to occur in three phases, an initial phase during which no stable form I crystals can be detected, a secondary phase characterized by a rapid form II dissolution and a mass increase of form I crystals, and a final phase during which form II crystals are no longer present and the solution tends towards the form I saturation concentration. Identification and understanding of each of these phases require knowledge of the nature of the crystallographic form, the solute concentration in solution, as well as the variations in particle size distributions, showing the necessity of combining the different online analyzers.

■ ASSOCIATED CONTENT

Supporting Information. Measurement principles of the Raman probe, the FBRM probe (Figure SI.1) and the ATR-FTIR probe: principle of the ATR technology (Figure SI.2), and calibration model of the ATR-FTIR probe (Figure SI.3). This material is available free of charge via the Internet at http://pubs.acs.org.

■ AUTHOR INFORMATION

Corresponding Author

*E-mail: christelle.herman@ulb.ac.be. Telephone: 0032 2 650 29 18. Fax: 0032 2 650 29 10.

■ ACKNOWLEDGMENT

C. Herman acknowledges technical support from UCB Pharma, based in Braine l'Alleud, Belgium, and financial support from the David et Alice Van Buuren funds, Emile Defay funds and the Fonds National de la Recherche Scientifique (F.R.S.-F.N.R.S.), Belgium.

■ REFERENCES

(1) Mersmann, A. *Crystallization Technology Handbook*, Marcel Dekker: New York, 1995.
(2) Mullin, J. W. *Crystallization*, 4th ed.; Elsevier: Amsterdam, 2001.
(3) Mangin, D.; Puel, F.; Veesler, S. *Org. Process Res. Dev.* **2009**, *13*, 1241–1253.
(4) Barret, P.; Smith, B.; Worlitschek, J.; Bracken, V.; O'Sullivan, B.; O'Grady, D. *Org. Process Res. Dev.* **2005**, *9*, 348–355.
(5) Févotte, G. *Int. J. Pharm.* **2002**, *241*, 263–278.
(6) De Smet, K.; van Dun, J.; Stokbroekx, B.; Spittaels, T.; Schroyen, C.; Van Broeck, P.; Lambrechts, J.; Van Cleuvenbergen, D.; Smout, G.; Dubois, J.; Horvath, A.; Verbraeken, J.; Cuypers, J. *Org. Process Res. Dev.* **2005**, *9*, 344–347.

(7) Wang, F.; Wachter, J. A.; Antosz, F. J.; Berglund, K. A. *Org. Process Res. Dev.* **2004**, *4*, 391–395.
(8) Barthe, S. C.; Grover, M. A.; Rousseau, M.; R.W. *J. Cryst. Growth Des.* **2008**, *8* (9), 3316–3322.
(9) Kobayashi, R.; Fujimaki, Y.; Ukita, T.; Hiyama, Y. *Org. Process Res. Dev.* **2006**, *10*, 1219–1226.
(10) Jia, C.-Y.; Yin, Q.-X.; Zhang, M.-J.; Wang, J.-K.; Shen, Z.-H. *Org. Process Res. Dev.* **2008**, *12*, 1223–1228.
(11) O'Sullivan, B.; Barret, P.; Hsiao, G.; Carr, A.; Glennon, B. *Org. Process Res. Dev.* **2003**, *7* (6), 977–982.
(12) O'Sullivan, B.; Glennon, B. *Org. Process Res. Dev.* **2005**, *9*, 884–889.
(13) Scholl, J.; Bonalumi, D.; Vicum, L.; Mazzotti, M. *J. Cryst. Growth Des.* **2006**, *6* (4), 881–891.
(14) Herman, C.; Leyssens, T.; Vermylen, V.; Halloin, V.; Haut, B. *J. Therm. Anal. Calorim.* **2011**, DOI: 10.1007/s10973-011-1555-0.
(15) Herman, C.; Leyssens, T.; Vermylen, V.; Halloin, V.; Haut, B. *J. Chem. Thermodynam.* **2011**, *43*, 677–682.
(16) Herman, C; Leyssens, T.; Debaste, F.; Haut, B. *J. Cryst. Growth* **2011**, DOI: 10.1016/j.jcrysgro.2011.04.009.
(17) Herman, C.; Haut, B.; Halloin, V.; Vermylen, V.; Leyssens, T. *Org. Process Res. Dev.* **2011**, *15*(4) 774−782
(18) Gamberini, M. C.; Baraldi, C.; Rustichelli, C.; Ferioli, V.; Gamberini, G. *J. Mol. Struct.* **2006**, *785*, 216–224.
(19) Starbuck, C.; Spartalis, A.; Wai, L.; Wang, J.; Fernandez, P.; Lindemann, C. M.; Zhou, G. X.; Ge, Z. *J. Cryst. Growth Des.* **2002**, *2* (6), 515–522.
(20) Wu, W.; Mehrman, S. J.; Zhou, Y.; Pu, S. X.; Huang, L.; Fermier, A.; Karki, S. *J. Cryst. Growth* **2009**, *311*, 3435–3444.
(21) Barret, P.; Glennon, B. *Trans IChemE* **2002**, *80* (A), 799–805.
(22) Barthe, S. DEA Thesis, Georgia Institute of Technology, 2006
(23) Méndez del Rio, J. R. PhD Thesis, Georgia Institute of Technology, 2004
(24) Worlitschek, J.; de Buhr, J. *Crystallization Studies with Focused Beam Reflectance Measurement and Multimax*, Application Note, AutoChem, MultiMax, Mettler Toledo: Columbia, MD, U.S.A., 2005
(25) Barret, P.; Glennon, B. *Part. Part. Syst. Char.* **1999**, *16*, 207–211.
(26) Leyssens, T.; Baudry, C.; Escudero-Hernandez, M. L. *Org. Process Res. Dev* **2011**, *15* (2), 413–426.
(27) Görnet, M.; Sadowski, G. *Macromol. Symp.* **2007**, *259*, 236–242.
(28) *ATR: Theory and Application*, Application Note 0402; Pike Technologies: Madison, WI, U.S.A.
(29) Teychené, S. PhD Thesis, Institut National Polytechnique de Toulouse, 2004
(30) Liotta, V.; Sabesan, V. *Org. Process Res. Dev.* **2004**, *8*, 488–494.
(31) Feng, L.; Berglund, K. A. *J. Cryst. Growth* **2002**, *2* (5), 449–452.
(32) Næs, T.; Isaksson, T.; Fearn, T.; Davies, T. *A User-Friendly Guide to Multivariate Calibration and Classification*; NIR Publications: Chichester, 2002.
(33) Garrido, M.; Larrechi, M. S.; Rius, F. X. *Anal. Chim. Acta* **2007**, *585*, 277–285.
(34) Nordström, F. L.; Rasmuson, A. C. *Eur. J. Pharm. Sci.* **2006**, *28*, 377–384.
(35) Mersmann, A.; Bartosch, K. *J. Cryst. Growth* **1998**, *183*, 240–250.
(36) Ulrich, J.; Strege, C. *J. Cryst. Growth* **2002**, *237−239*, 2130–2135.
(37) Davey, R. J.; Guy, P. D.; Ruddick, A. J. *J. Colloid Interface Sci.* **1985**, *108* (1), 189–192.
(38) Cardew, P. T.; Davey, R. J. *Proc. R. Soc. Lond.* **1985**, *398*, 415–428.
(39) Garcia, E.; Veesler, S.; Boistelle, R.; Hoff, C. *J. Cryst. Growth* **1999**, *198−199*, 1360–1364.
(40) Garcia, E.; Hoff, C.; Veesler, S. *J. Cryst. Growth* **2002**, *237−239*, 2233–2239.
(41) Gu, C.-H.; Young, V., Jr.; Grant, D. J. W. *J. Pharm. Sci.* **2001**, *90* (11), 1878–1890.